ORIGINAL PAPER

CrossMark

An analytical model for multiple fractured shale gas wells considering fracture networks and dynamic gas properties

Yongchao Xue[1] · Yonghui Wu[1] · Linsong Cheng[1] · Shijun Huang[1] · Shuang Ai[2] · Yanwei Yang[1]

Abstract

Multi-stage fractured horizontal wells play an important role in developing shale gas reservoirs by significantly improving productivity. By considering fracture networks, gas desorption, stress-sensitive fracture permeability, and pressure-dependent gas PVT properties, an analytical model is developed for shale gas wells. Fracture networks are handled based on transient linear flow, gas desorption is handled by defining a new total compressibility, stress-dependent hydraulic fracture permeability is handled by variable substitution, and pseudo-pressure and pseudo-time are used to handle pressure-dependent PVT properties. After obtaining the solution of the linearized model, a material balance method and successive substitution iteration procedure are proposed to convert the pseudo-time into real time and calculate the production contribution from gas desorption. The results show that induced fractures also have a great impact on the production of the well. Production contribution from free gas and adsorbed gas could be quantified using the proposed material balance principle and iterative method. The rank of parameters that influence the ultimate recovery is the following: half-length of hydraulic fracture, induced fracture length/hydraulic fracture spacing, hydraulic fracture spacing, conductivity of induced fractures, conductivity of hydraulic fracture, and induced fracture spacing.

Keywords Shale gas · Fracture networks · Analytical model · Dynamic gas property · Gas desorption

Introduction

Shale gas is an unconventional natural gas resource which is hard to develop, and its commercial development requires multi-stage fracture and high investment. It is of great theoretical and practical significance to develop productivity evaluation methods and investigate major factors affecting the productivity of multi-stage fractured horizontal well in shale gas reservoirs.

To handle the fracture networks after hydraulic fracturing, several semi-analytical models based on boundary element method and Green's function are proposed (Jia et al. 2016; Chen et al. 2016; Cheng et al. 2017; He et al. 2017; Zhang

et al. 2018). And to further consider pressure-dependent gas PVT properties and dynamic gas desorption, many numerical methods are applied (Mayerhofer et al. 2010; Wu et al. 2013; Zhang et al. 2015; Mi et al. 2017).

Bello and Wattenbarger (2010) established a dual-porosity slab model for multi-stage fractured horizontal shale gas wells, made type curves of production rate, and classified gas flow regimes into matrix linear flow, bilinear flow, linear flow in natural fractures, and boundary-influenced flow from matrix into well. Al-Ahmadi and Wattenbarger (2011) introduced natural fractures and hydraulic fractures into the dual-porosity slab model, assuming that hydraulic fractures are perpendicular to well while natural fractures are parallel with the well, and he presented the productivity evaluation model of linear flow in triple media. Tivayanonda et al. (2012) considered that conductivity in hydraulic fractures is much greater than that in natural fractures, making further simplification of Al-Ahmadi's model by regarding conductivity in hydraulic fractures as infinite conductivity. Ozkan et al. (2011) presented the concept of trilinear flow and classified the whole reservoir into the SRV inner zones between hydraulic

✉ Yonghui Wu
   wuyonghuijr@gmail.com

[1] Department of Petroleum Engineering, China University of Petroleum, Beijing, China

[2] Petroleum Engineering Technology Research Institute, China Petrochemical Corporation, Beijing, China

fractures and the SRV outer zones without being fractured. The SRV inner zones completely consist of dual porosity and the SRV outer zones only consist of single porosity. Brohi et al. (2011) made type curves of non-steady trilinear flow, on the condition of constant borehole pressure (BHP) coupled with constant pressure of outer boundary or closed outer boundary respectively. Xu et al. (2013) considered that horizontal shale gas wells treated with stimulated reservoir volume (SRV) could be represented by dual-porosity slab multiple linear flow model in outer and inner zone, and he derived non-steady productivity equations on the condition of constant BHP. Stalgorova and Mattar (2013) considered that SRV inner zones were not completely of dual porosity but fractures in SRV inner zones were of single porosity, and he presented the model indicating that along the length of horizontal well were not completely fractured dual-porosity zones, and non-fractured zones existed between different fractured zones along the well, which supplied fluid to SRV inner zones in the form of linear flow as SRV outer zones at the end of fractures.

However, aforementioned studies failed to include stress sensitivity of hydraulic fractures and nonlinear factors such as nonlinear desorption and PVT properties. In this paper, we proposed an analytical model for multi-stage fractured horizontal wells from shale gas reservoirs to obtain the performance. Fracture networks, gas desorption, stress-sensitive fracture permeability, and pressure-dependent gas PVT properties are considered in the analytical model. Then a material balance method and a successive iteration procedure are proposed to obtain gas production vs. time and production contribution of desorbed gas. Finally, the effects of different model parameters on shale gas production and production composition are investigated.

Physical model

Multi-stage fractured horizontal well is important for efficient exploitation of shale reservoirs, especially the horizontal well with SRV, which tremendously increases the productivity of shale gas producers. As shown in Fig. 1, in the shale formation where stratification and lamellae are well developed (such as the lower part of Longmaxi formation in Southwest China), complicated small-scale fracture networks can be established after being fractured, and productivity is better than before. This paper presents the productivity evaluation model with fracture networks for the shale reservoirs where stratification and lamellae are undeveloped. Other assumptions are shown below:

a. The formation is assumed to be horizontal, with the same thickness and fully penetrated by the hydraulic fractures.
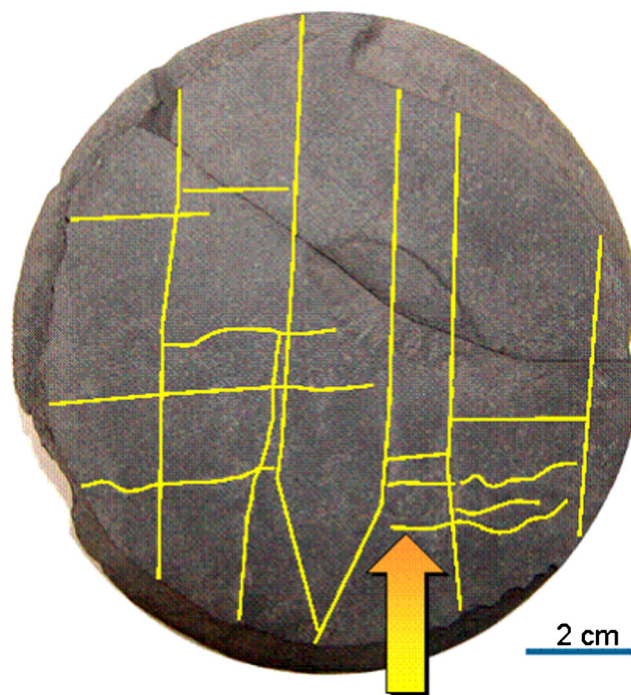

Fig. 1 A shale core from Longmaxi formation in South China

b. Each zone of the model shown in Fig. 2 is assumed to be heterogeneous and isotropic.
c. Single-phase gas is considered for flow in the formation, and gravity effect is neglected.
d. Langmuir adsorption is used to characterize shale gas adsorption in the matrix, and gas desorption is also assumed to obey the Langmuir isotherm.

In this paper, the induced fractures are assumed to be perpendicular to the planner hydraulic fractures to derive the analytical solution of the model, as shown in Fig. 2. The flow in each region for the model is assumed to be linear. Gas in the outer zone is assumed to be linearly flow into the hydraulic fractures. There is a skin factor because of the convergence flow in to the fractures. Gas in shale matrix of inner zone linearly flows into induced fractures, and then gas in the
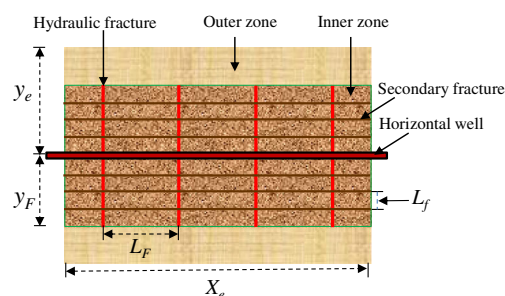

Fig. 2 Physical model for multi-stage fractured horizontal shale gas wells with fracture networks

induced fractures linearly flows into the hydraulic fractures. Eventually, gas in the hydraulic fractures flows into the horizontal well linearly along the fracture.

Mathematical model

Mathematical model with fracture networks

For gas flow in the formation, pseudo-pressure and pseudo-time (Gerami et al. 2008) are often used the handle the gas PVT properties and respectively defined as

$$\psi_m = 2 \int_0^{p_m} \frac{p_m}{\mu Z} dp_m \tag{1}$$

$$t_a = \int_0^t \frac{\mu_{gi} c_{tmi}}{\mu_g(\overline{p}_m) c_{tm}(\overline{p}_m)} dt \tag{2}$$

According to assumptions, as shown in Fig. 2, using the dimensionless variables shown in Table 1, the model of outer zone can be represented in dimensionless form as follows:

$$\begin{cases} \dfrac{\partial^2 \psi_{oD}}{\partial y_D^2} = \eta_D \dfrac{\partial \psi_{oD}}{\partial t_D} \\[2mm] \psi_{oD}(y_D, t_D)\big|_{t_D=0} = 0 \\[2mm] \psi_{FD}(y_D, t_D)\big|_{y_D=y_{FD}} = \psi_{oD}(y_D, t_D)\Big|_{y_D=y_{FD}} + s_c \\[2mm] \dfrac{\partial \psi_{FD}(y_D, t_D)}{\partial y_D}\bigg|_{y_D=y_{FD}} = \dfrac{1}{\xi} \dfrac{\partial \psi_{oD}(y_D, t_D)}{\partial y_D}\bigg|_{y_D=y_{FD}} \\[2mm] \psi_{oD}(y_D, t_D)\big|_{y_D \to \infty} = 0 \end{cases} \tag{3}$$

It should be noticed that the s_c in the model is considering the convergence flow effect when gas flows from the outer zone to the fracture tips.

Given that gas flows in the form of matrix nonlinear flow and along the direction of Z axis, from matrix into induced fractures, coupled with desorption of absorbed gas in shale matrix and three migration mechanisms of gas in nanoscaled porosity, the model of inner matrix can be expressed as follows:

$$\begin{cases} \dfrac{\partial^2 \psi_{mD}}{\partial z_D^2} = \dfrac{3\omega_m}{\lambda_{fm}} \dfrac{\partial \psi_{mD}}{\partial t_D} \\[2mm] \psi_{mD}(z_D, t_D)\big|_{t_D=0} = 0 \\[2mm] \dfrac{\partial \psi_{mD}(z_D, t_D)}{\partial z_D}\bigg|_{z_D=0} = 0 \\[2mm] \psi_{mD}(z_D, t_D)\big|_{z_D=1} = \psi_{fD} \end{cases} \tag{4}$$

Similar to the flow model for gas flow from shale matrix into the induced fracture systems, and considering the flux contribution from shale matrix, the dimensionless form of equations of induced fracture can be expressed as follows:

$$\begin{cases} \dfrac{\partial^2 \psi_{fD}}{\partial x_D^2} = \dfrac{3\omega_f}{\lambda_{fm}} \dfrac{\partial \psi_{fD}}{\partial t_D} - \dfrac{\lambda_{fm}}{\lambda_{Ff}} \dfrac{\partial \psi_{mD}}{\partial z_D}\bigg|_{z_D=1} \\[2mm] \psi_{fD}(x_D, t_D)\big|_{t_D=0} = 0 \\[2mm] \dfrac{\partial \psi_{fD}(x_D, t_D)}{\partial x_D}\bigg|_{x_D=0} = 1 \\[2mm] \psi_{fD}(x_D, t_D)\big|_{x_D=1} = \psi_{FD} \end{cases} \tag{5}$$

Considering the gas contribution from the induced fracture systems, and coupling the flow with the outer zone, the dimensionless form of hydraulic fracture model can be expressed as follows:

$$\begin{cases} \dfrac{\partial^2 \psi_{FD}}{\partial y_D^2} = \omega_F \dfrac{\partial \psi_{FD}}{\partial t_D} - \dfrac{\lambda_{Ff}}{3} \dfrac{\partial \psi_{fD}}{\partial x_D}\bigg|_{x_D=1} \\[2mm] \psi_{FD}(y_D, t_D)\big|_{t_D=0} = 0 \\[2mm] \psi_{FD}(y_D, t_D)\big|_{y_D=0} = 1 \\[2mm] \psi_{FD}(y_D, t_D)\big|_{y_D=y_{FD}} = \psi_{oD}(y_D, t_D)\Big|_{y_D=y_{FD}} + s_c \\[2mm] \dfrac{\partial \psi_{FD}(y_D, t_D)}{\partial y_D}\bigg|_{y_D=y_{FD}} = \dfrac{1}{\xi} \dfrac{\partial \psi_{oD}(y_D, t_D)}{\partial y_D}\bigg|_{y_D=y_{FD}} \end{cases} \tag{6}$$

Handling gas desorption and stress sensitivity of fracture permeability

In the matrix of shale gas reservoirs, the continuity equation incorporating desorption is given below:

$$\frac{\partial}{\partial x}(-\rho v) = \frac{\partial(\rho \phi)}{\partial t} + \rho B_g \frac{\partial V}{\partial t} \tag{7}$$

The second term on the right side of Eq. (7) represents the influx into fractures from matrix due to desorption. In this paper, the Langmuir isotherm model is used:

$$V = \frac{V_L p}{p_L + p} \tag{8}$$

Substituting gas and pore compressibility and Eq. (8) into Eq. (7), to arrive at

$$\frac{\partial^2 \psi}{\partial x^2} = \frac{\phi \mu}{k} \left[c_m + c_g + \frac{Z p_{sc} T}{\phi Z_{sc} T_{sc}} \frac{V_L p_L}{p(p_L + p)^2} \right] \frac{\partial \psi}{\partial t} \tag{9}$$

Desorption compressibility (Bumb and McKee 1988; Wu et al. 2016) is a good method to handle gas desorption:

$$c_d = \frac{p_{sc}ZT}{\phi Z_{sc}T_{sc}} \frac{V_L p_L}{p(p_L + p)^2} \tag{10}$$

Substituting Eqs. (1), (2), and (10) into Eq. (9), the diffusivity equation becomes:

$$\frac{\partial^2 \psi}{\partial x^2} = \frac{\phi \mu_{gi} c_{ti}}{0.0864k} \frac{\partial \psi}{\partial t_a} \tag{11}$$

The format of Eq. (11) is the same as diffusivity equations of conventional gas flow model.

Many experimental tests show that stress sensitivity is strong in shale formation (Guo et al. 2012; Zhao et al. 2013). And permeability of hydraulic fracture shows a good exponential relationship with effective stress under the overburden pressure (Huang et al. 2018). Pseudo-permeability γ_F of hydraulic fracture can be introduced into the model and expressed as follows:

$$\gamma_F = \frac{1}{k_F} \frac{dk_F}{d\psi} \tag{12}$$

Pseudo-pressure of hydraulic fracture can be shown as follows:

$$k_F = k_{Fi}e^{\gamma_F(\psi_F - \psi_i)} \tag{13}$$

k_{Fi} represents permeability of hydraulic fractures without overburden pressure, mD. γ_F represents pseudo-permeability of hydraulic fractures, (mPa·s)/(MPa)^2. $\psi_i - \psi_F$ represents pseudo-effective stress of hydraulic fractures, (MPa)^2/(mPa·s).

Given that the quadratic term of pressure gradient on the left hand of equation is nonlinear, an intermediate variable is introduced and expressed as follows (Huang et al. 2018):

$$\psi_{FD} = -\frac{1}{\gamma_{FD}} \ln[1 - \gamma_{FD} \cdot \eta_F] \tag{14}$$

After changing the equation with intermediate variable, the nonlinear right hand of equation can be changed with regular perturbation method. With the use of Taylor expansion, the right hand can be changed as follows:

$$\frac{1}{1 - \gamma_{FD}\eta_F(y_D, t_D)} = 1 + \gamma_{FD}\eta_F(y_D, t_D) + \gamma_{FD}^2\eta_F^2(y_D, t_D) + \cdots\cdots \tag{15}$$

For $\gamma_{FD} \cdot \eta_F \ll 1$ and it is extremely small, the zero order perturbation solution is accurate. So the first term on right hand should be kept to simplify the whole equation, and the model of hydraulic fracture can be simplified as follows:

$$\begin{cases} \dfrac{\partial^2 \eta_F}{\partial y_D^2} = \omega \dfrac{\partial \eta_F}{\partial t_D} - \dfrac{\lambda_{cw}}{3}\left|\dfrac{\partial \psi_{mD}}{\partial x_D}\right|_{x_D=1} \\[2mm] \eta_F(y_D, t_D)|_{t_D=0} = 0 \\[2mm] \eta_F(y_D, t_D)|_{y_D=0} = \dfrac{1}{\gamma_{FD}}(1 - e^{-\gamma_{FD}}) \\[2mm] \dfrac{\partial \eta_F(y_D, t_D)}{\partial y_D}\bigg|_{y_D=y_{FD}} = \dfrac{1}{\xi}\dfrac{\partial \psi_{oD}(y_D, t_D)}{\partial y_D}\bigg|_{y_D=y_{FD}} \\[2mm] \eta_F(y_D, t_D)|_{y_D=y_{FD}} = \psi_{oD}(y_D, t_D)\bigg|_{y_D=y_{FD}} + s_c \end{cases} \tag{16}$$

It should be noticed that the model considering stress sensitive fracture permeability shown in Eq. (16) is similar to Eq. (6); the only difference is that the dimensionless pseudo-pressure ψ_{FD} in Eq. (6) is replaced by the intermediate variable η_F.

Table 1 Definition of dimensionless variables

Variables	Definition	Variables	Definition
Dimensionless rate	$\dfrac{1}{q_D} = \dfrac{k_F\sqrt{A_{cw}}(\psi_i - \psi_{wf})}{1.291\times10^{-3}q_{sc}T}$	Dimensionless pseudo-pressure	$\psi_D = \dfrac{\psi_i - \psi}{\psi_i - \psi_{wf}}$
Dimensionless time	$t_D = \dfrac{0.0864k_F t_a}{\mu(\phi_m c_{tm} + \phi_f c_{tf} + \phi_F c_{tF})A_{cw}}$	Dimensionless flow coefficient	$\xi = \dfrac{A_F k_F}{A_o k_o}$
Diffusivity ratio	$\eta_D = \dfrac{\eta_F}{\eta_o} = \dfrac{k_F}{\phi_m c_{tm} + \phi_f c_{tf} + \phi_F c_{tF}}\dfrac{\phi_o c_{to}}{k_o}$	Dimensionless length -X direction	$x_D = \dfrac{x}{L_F/2}$
Storativity ratio of shale matrix	$\omega_m = \dfrac{\phi_m c_{tm}}{\phi_m c_{tm} + \phi_f c_{tf} + \phi_F c_{tF}}$	Dimensionless length -Y direction	$y_D = \dfrac{y}{\sqrt{A_{cw}}}$
Storativity ratio of shale induced fractures	$\omega_f = \dfrac{\phi_f c_{tf}}{\phi_m c_{tm} + \phi_f c_{tf} + \phi_F c_{tF}}$	Dimensionless fracture half-length	$y_{FD} = \dfrac{y_F}{\sqrt{A_{cw}}}$
Storativity ratio of shale hydraulic fractures	$\omega_F = \dfrac{\phi_F c_{tF}}{\phi_m c_{tm} + \phi_f c_{tf} + \phi_F c_{tF}}$	Dimensionless distance to boundary	$y_{eD} = \dfrac{y_e}{\sqrt{A_{cw}}}$
Interporosity flow coefficient between inner reservoir and fracture	$\lambda_{IF} = \dfrac{12}{L_F^2}\dfrac{k_I}{k_F}A_{cw}$		
Interporosity flow coefficient between matrix and induced fracture	$\lambda_{fm} = \dfrac{12}{L_f^2}\dfrac{k_m}{k_F}A_{cw}$	Interporosity flow coefficient between inner reservoir and fracture	$\lambda_{Ff} = \dfrac{12}{L_f^2}\dfrac{k_f}{k_F}A_{cw}$

Fig. 3 Flow chart of iteration for production composition model for fractured horizontal wells in shale reservoir
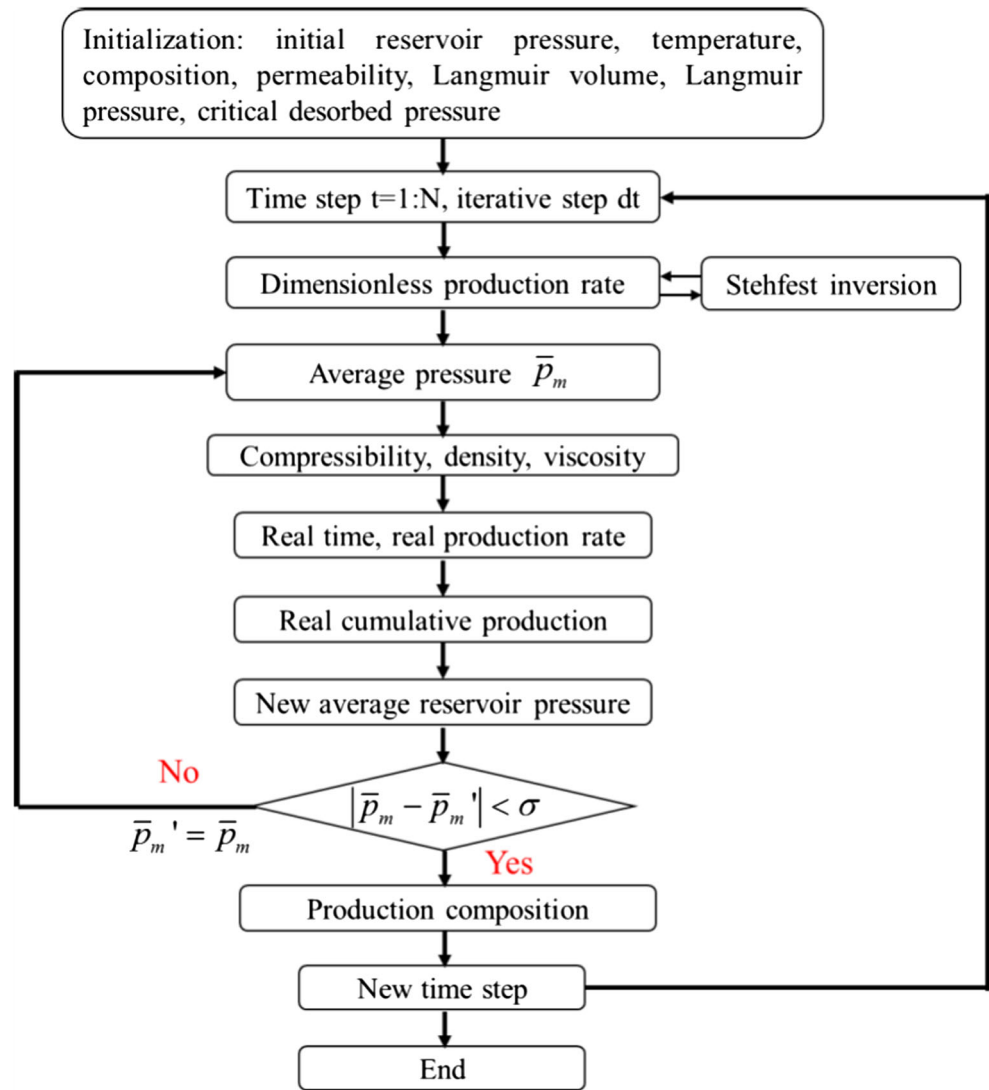

Table 2 Parameters for calculation of productivity of horizontal wells with fracture networks

Variable	Value	Variable	Value
Original reservoir pressure, MPa	50.75	BHP, MPa	30
Reservoir temperature, K	367.65	Reservoir thickness, m	46
Horizontal well length, m	1200	Amount of hydraulic fractures	10
Half-length of primary fracture, m	200	Width of primary fracture, m	5×10^{-3}
Langmuir pressure, MPa	5.82	Langmuir volume, m^3/m^3	9.26
Permeability of inner matrix, mD	4×10^{-4}	Permeability of outer matrix, mD	8×10^{-5}
Porosity of inner matrix	0.05	Porosity of outer matrix	0.05
Pore compressibility of matrix in inner and outer zone, MPa^{-1}	8×10^{-5}	Compressibility of primary fracture, MPa^{-1}	1×10^{-4}
Width of productive zone, m	70	Gas relative density	0.6915
Permeability of fissure in inner zone, mD	0.4	Permeability of fissure in outer zone, mD	0.1
Permeability of induced fractures, mD	20	Width of induced fractures, m	5×10^{-4}
Compressibility of induced fractures, MPa^{-1}	1×10^{-4}	Spacing of induced fractures, m	100

Fig. 4 The effect of inner zone fissure aperture on horizontal wells productivity with fracture networks

(a) Production rate

(b) Cumulative production
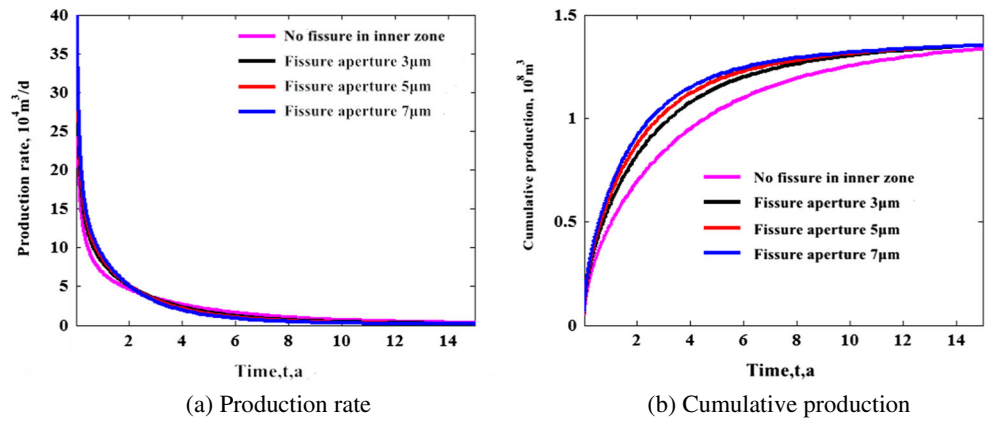
Solution of the model

On the condition of constant BHP, gas flows into well in the form of linear flow in hydraulic fractures, and dimensionless productivity of fractured horizontal shale gas well with fracture networks can be expressed as follows:

$$q_D = -\frac{1}{2\pi} \left. \frac{\partial \psi_F(y_D, t_D)}{\partial y_D} \right|_{y_D=0} \quad (17)$$
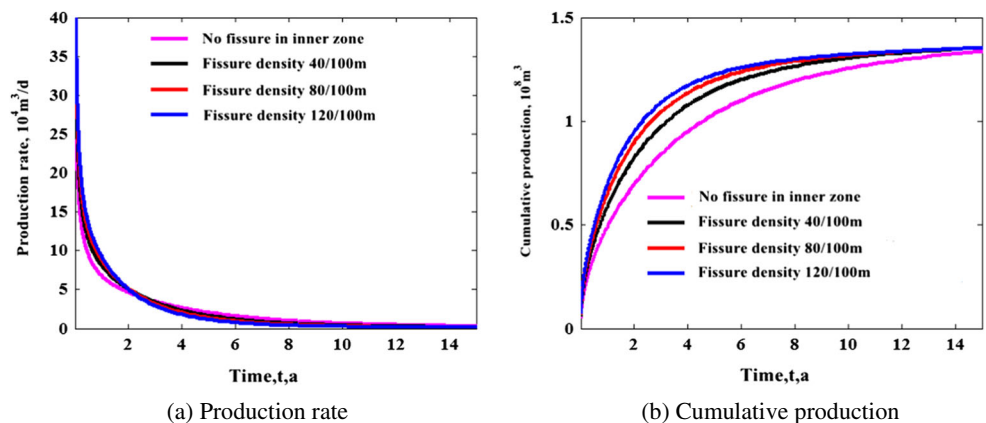
Given stress sensitivity of hydraulic fractures, dimensionless productivity of fractured horizontal shale gas well with fracture networks can be expressed as follows:

$$q_D = -\frac{1}{2\pi} \left. \frac{\partial \eta_F(y_D, t_D)}{\partial y_D} \right|_{y_D=0} \quad (18)$$

With the use of Laplace transformation, the general solution of aforementioned model with finite outer boundary can be achieved in the Laplace space. Associated with initial conditions and boundary conditions, productivity of fractured horizontal shale gas well with fracture networks can be expressed as follows:

$$\overline{q}_D = \frac{\sqrt{sf(s)}}{2\pi s} \frac{1 - e^{-\gamma_{FD}}}{\gamma_{FD}} \frac{I + M}{N + O} \quad (19)$$

where

$$I = \frac{\sqrt{s\eta_D}}{\xi} \left[e^{2\sqrt{s\eta_D} \cdot y_{eD}} - e^{2\sqrt{s\eta_D} \cdot y_{FD}} \right] \left\{ \cosh \left[\sqrt{sf(s)} \cdot y_{FD} \right] - s_c \frac{\gamma_{FD}}{1 - e^{-\gamma_{FD}}} \right\} \quad (20)$$

$$M = \left[e^{2\sqrt{s\eta_D} \cdot y_{eD}} + e^{2\sqrt{s\eta_D} \cdot y_{FD}} \right] \sqrt{sf(s)} \sinh \left[\sqrt{sf(s)} \cdot y_{FD} \right] \quad (21)$$

$$N = \frac{\sqrt{s\eta_D}}{\xi} \left[e^{2\sqrt{s\eta_D} \cdot y_{eD}} - e^{2\sqrt{s\eta_D} \cdot y_{FD}} \right] \sinh \left[\sqrt{sf(s)} \cdot y_{FD} \right] \quad (22)$$

$$O = \left[e^{2\sqrt{s\eta_D} \cdot y_{eD}} + e^{2\sqrt{s\eta_D} \cdot y_{FD}} \right] \sqrt{sf(s)} \cosh \left[\sqrt{sf(s)} \cdot y_{FD} \right] \quad (23)$$

In which, $f(s)$ is defined as

$$\begin{cases} f(s) = \omega_F + \dfrac{\lambda_{Ff}}{3s} \sqrt{sf_f(s)} \tanh \left[\sqrt{sf_f(s)} \right] \\ f_f(s) = \dfrac{3\omega_f}{\lambda_{Ff}} + \dfrac{\lambda_{fm}}{\lambda_{Ff}} \sqrt{\dfrac{3\omega_m}{\lambda_{fm}s}} \tanh \sqrt{\dfrac{3s\omega_m}{\lambda_{fm}}} \end{cases} \quad (24)$$

If skin ($s_c = 0$) and production of outer matrix ($\xi \to \infty$, $y_{eD} = y_{FD}$) are not taken into account, the productivity equations of fracture networks model could be written as

$$\overline{q}_D = \frac{\sqrt{sf(s)}}{2\pi s} \tanh \left[\sqrt{sf(s)} \cdot y_{eD} \right] \quad (25)$$

Equation (25) is identical to that of Al-Ahmadi and Wattenbarger (2011); this validates the productivity model of horizontal well with fracture networks in this paper.

Fig. 5 The effect of inner zone fissure density on horizontal wells productivity with fracture networks

(a) Production rate

(b) Cumulative production

Fig. 6 The effect of hydraulic fractures half-length on horizontal wells productivity with fracture network

(a) Production rate   (b) Cumulative production
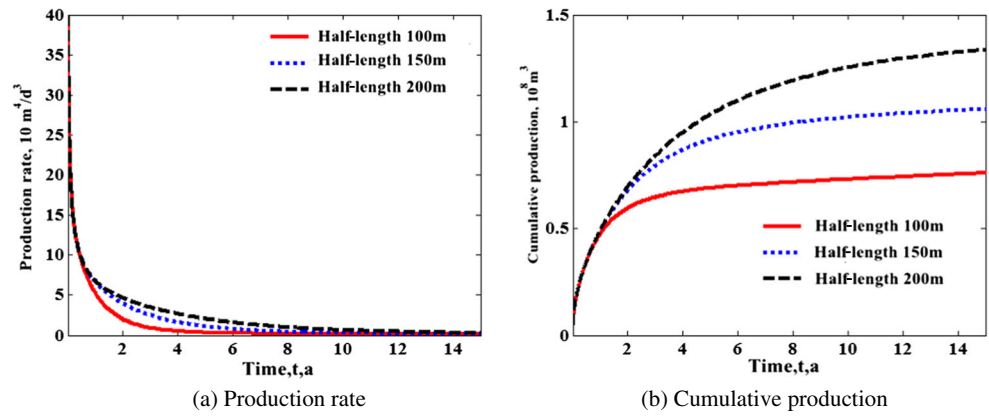
Production prediction considering pressure-dependent gas PVT properties

Owing to extremely low permeability of shale matrix, pressure systems of two adjacent wells can hardly connect with each other. Thus, each fractured horizontal well can be regarded as an independent gas reservoir with artificial treatment. Material balance principle of gas reservoir engineering can be utilized to determine the average reservoir pressure in different moments:

$$\frac{\overline{p}_m}{Z\left(\overline{p}_m\right)} = \frac{p_i}{Z(p_i)}\left(1 - \frac{G_P}{G}\right) \tag{26}$$

Table 3 Experimental design and calculated results for fractures network model

Parameter	Half-length of hydraulic fracture, m	Conductivity of hydraulic fracture, mD·m	Hydraulic fracture spacing, m	Conductivity of induced fractures, mD·m	Induced fracture spacing, m	Induced fracture length/hydraulic fracture spacing	Cumulative production in 20 years, 10^8 m^3	Average production in the first year, 10^4m^3/day
Case 1	100	0.5	25	0.01	10	1	1.43	27.3
Case 2	100	1	30	0.05	15	0.9	1.37	25.5
Case 3	100	2	35	0.1	20	0.8	1.41	23.7
Case 4	100	3	40	0.15	25	0.7	1.43	20.8
Case 5	100	4	45	0.2	30	0.6	1.43	18.5
Case 6	150	0.5	30	0.1	25	0.6	1.99	24.8
Case 7	150	1	35	0.15	30	1	1.73	24.5
Case 8	150	2	40	0.2	10	0.9	2.00	28.3
Case 9	150	3	45	0.01	15	0.8	2.09	25.1
Case 10	150	4	25	0.05	20	0.7	2.06	34.3
Case 11	200	0.5	35	0.2	15	0.7	2.52	26.0
Case 12	200	1	40	0.01	20	0.6	2.57	24.1
Case 13	200	2	45	0.05	25	1	2.73	24.5
Case 14	200	3	25	0.1	30	0.9	2.70	36.5
Case 15	200	4	30	0.15	10	0.8	2.55	34.8
Case 16	250	0.5	40	0.05	30	0.8	3.08	22.8
Case 17	250	1	45	0.1	10	0.7	3.27	26.1
Case 18	250	2	25	0.15	15	0.6	3.29	37.9
Case 19	250	3	30	0.2	20	1	3.15	34.2
Case 20	250	4	35	0.01	25	0.8	3.13	29.1
Case 21	300	0.5	45	0.15	20	0.9	3.61	23.1
Case 22	300	1	25	0.2	25	0.8	3.92	35.9
Case 23	300	2	30	0.01	30	0.7	3.75	31.5
Case 24	300	3	35	0.05	10	0.6	3.68	31.6
Case 25	300	4	40	0.1	15	1	3.84	30.3

Table 4   Mean and range of production rate in the first year for fractures network model

Parameters		Half-length of hydraulic fracture, m	Conductivity of hydraulic fracture, mD·m	Hydraulic fracture spacing, m	Conductivity of induced fractures, mD·m	Induced fracture spacing, m	Induced fracture length/hydraulic fracture spacing
Average production rate in the first year, $10^4 m^3$/day	Mean 1	23.17	24.82	34.38	27.43	29.63	28.16
	Mean 2	27.42	27.21	30.16	27.73	28.97	28.36
	Mean 3	29.18	29.20	27.00	28.31	27.88	28.57
	Mean 4	30.01	29.66	25.27	28.23	27.03	27.76
	Mean 5	30.49	29.38	23.47	28.58	26.77	27.38
	Range	7.32	4.84	10.92	1.15	2.87	1.18

In which, $\bar{p}_m$ means average matrix pressure in certain moment, MPa. p_i means initial matrix pressure, MPa. G_p and G means cumulative production and geological reserves.

As the application of Eq. (2), with the introduction of dimensionless pseudo-time, the model for fractured horizontal wells with fracture networks can be transformed into linear form, and their general solution of productivity is in the same form of linear solution. However, the calculated solution is on the condition of dimensionless pseudo-time, which means it must be transformed into real form.

Because changing real time into pseudo-time requires average pressure in different moments, and average pressure is associated with production rate as well as cumulative production which require pseudo-time for calculation, the whole calculated process of all parameters is closed and different parameters have mutual influence, requiring iterative method for solution. The process of iterative method is shown as Fig. 3.

1. Initialization of parameters including fundamental parameters of gas and reservoir.
2. With the use of general productivity equations of slab fractures or network model, calculating dimensionless production rate with Stefest numerical inversion in every dimensionless time step.
3. Assume average reservoir pressure as $\bar{p}_m$ in current time step.

4. Calculate gas physical parameters under current $\bar{p}_m$, including compressibility, density, and viscosity.
5. Calculate real time and real production rate with Eq. (19) and gas physical parameters.
6. Calculating real cumulative production.
7. Calculating new average reservoir pressure $\bar{p}_m'$ with Eq. (25).
8. Repeat steps from (3) to (7) until the difference of $\bar{p}'$ and last $\bar{p}_m$ meets requirement of accuracy.
9. Calculate composition of production rate in current time step with real average reservoir pressure.
10. Calculate the next time step until the whole calculating process ends.

If real average reservoir pressure is worked out, the proportion of desorbed gas can be calculated. Owing to depletion development of shale gas reservoir, the proportion of desorption compressibility equals to the proportion of desorbed gas. The proportion of absorbed gas production to the whole gas production can be represented as follows:

$$R_a = \frac{c_d\left(\bar{p}_m\right)}{c_{tm}\left(\bar{p}_m\right)} \times 100\% \qquad (27)$$

Table 5   Mean and range of recovery within 20 years for fractures network model

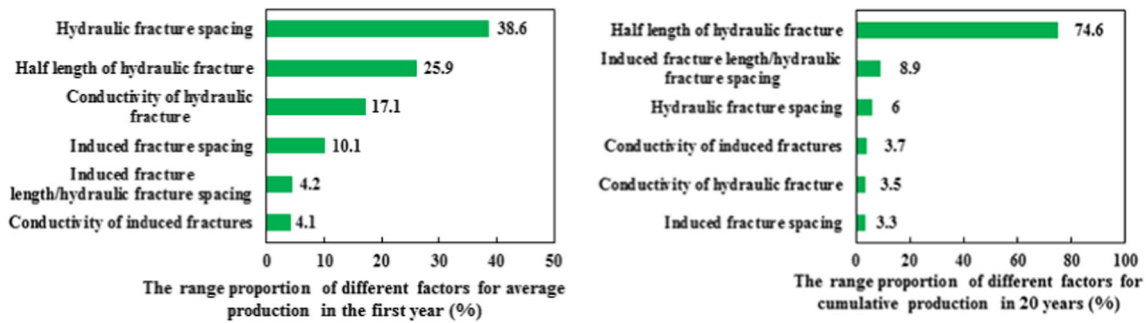| Parameters		Half-length of hydraulic fracture, m	Conductivity of hydraulic fracture, mD·m	Hydraulic fracture spacing, m	Conductivity of induced fractures, mD·m	Induced fracture spacing, m	Induced fracture length/hydraulic fracture spacing
Cumulative production in 20 years, 10^8 m^3	Mean 1	1.42	2.53	2.68	2.59	2.59	2.58
	Mean 2	1.98	2.57	2.56	2.58	2.62	2.42
	Mean 3	2.61	2.64	2.49	2.64	2.56	2.70
	Mean 4	3.19	2.61	2.58	2.52	2.64	2.61
	Mean 5	3.76	2.60	2.63	2.61	2.54	2.59
	Range	2.34	0.11	0.19	0.12	0.10	0.28

Fig. 7 The rank of parameters of initial production rate and recovery for fractures network model

Results and discussion

The effects of fracture parameters on production

With the use of model, we analyzed the effects of different parameters on gas production of the well. Parameters of the case are shown in Table 2.

The effect of inner zone fissure aperture on productivity of horizontal wells with fracture networks is shown as Fig. 4. It is apparent that higher fissure aperture leads to higher effective permeability of inner matrix, higher production rate in earlier stage as well as higher cumulative production.

The effect of inner zone fissure density on productivity of horizontal wells with fracture networks is shown as Fig. 5. It is clear that higher fissure density results in higher effective permeability of inner matrix, higher production rate in earlier stage, and higher cumulative production.

Figure 6 shows the effect of half-length of hydraulic fractures on productivity of horizontal wells with fracture network, on the condition of the same amount of induced fractures. If the number of induced fractures is the same, productivity of different fractured horizontal wells in earlier stage is of little difference. It is because that conductivity of primary

fracture can be regarded to be infinite, and initial production rate is mainly influenced by induced fractures. If primary fracture is longer, there will be more matrix directly connected with primary fracture, and production rate in later stage as well as cumulative production will be higher.

Production composition of model with fracture networks

In order to further clarify the effect of different parameters on initial production rate and recovery of fractured horizontal wells with fracture networks in shale reservoir, orthogonal experiments are implemented. Experimental parameters include permeability of matrix in outer and inner zone, half-length of hydraulic fractures, induced fractures spacing, width of inner zone, and SRV spacing. Each parameter has three different levels. With the introduction of one additional auxiliary parameter with one level, the final orthogonal experimental scheme can be set as shown in Table 3.

Cumulative production in 20 years and the average production rate in the first year can be calculated with parameters of orthogonal experimental scheme. What's more, cumulative
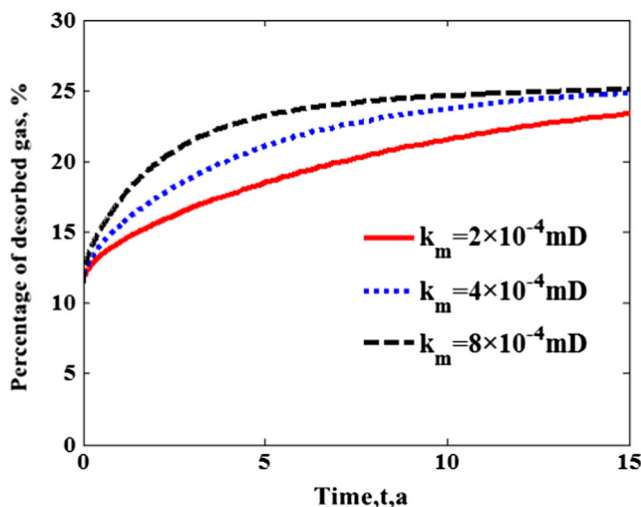

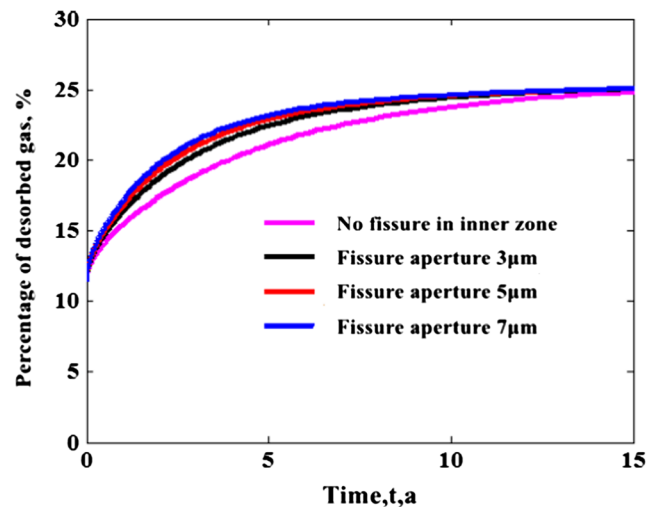**Fig. 8** The effect of matrix permeability of inner zone on production composition

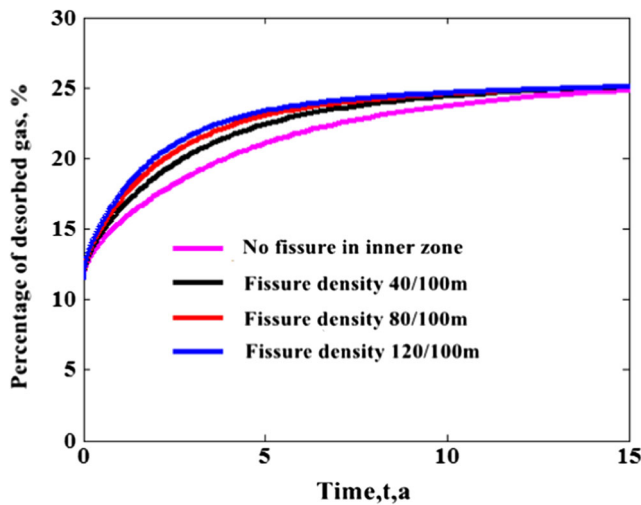**Fig. 9** The effect of fissure aperture of inner zone on production composition

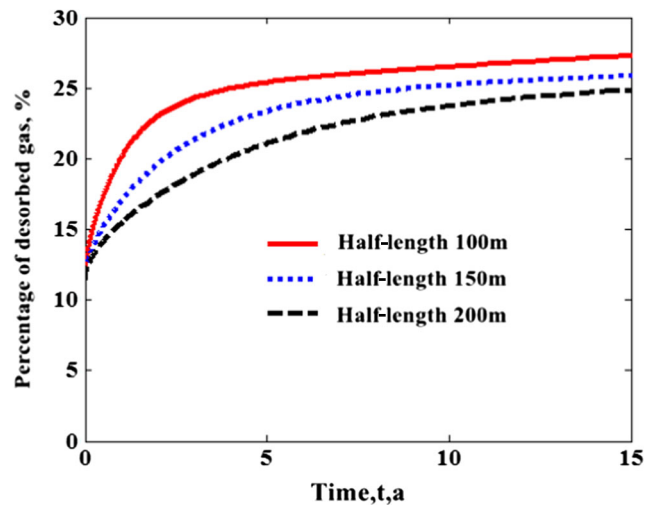**Fig. 10** The effect of fissure density of inner zone on production composition

Fig. 12 The effect of half-length of primary fracture on production composition

production in 20 years and the average production rate in the first year in different levels of all parameters can be worked out. The range represents the influence of different parameters on the average production rate in the first year and cumulative production in 20 years, which is shown in Tables 4 and 5. Figure 7 reveals the proportion of range of different parameters of the average production rate in the first year and the proportion of range of different parameters of cumulative production in 20 years.

It is apparent that the rank of parameters of the average production rate in the first year for fractures network model is the following: hydraulic fracture spacing > half-length of hydraulic fracture > conductivity of hydraulic fracture > induced fracture spacing > induced fracture length/hydraulic fracture spacing > conductivity of induced fractures. And the rank of parameters of cumulative production in 20 years is the following: half-length of hydraulic fracture > induced fracture

length/hydraulic fracture spacing > hydraulic fracture spacing > conductivity of induced fractures > conductivity of hydraulic fracture > induced fracture spacing.

Analysis of production contribution from desorbed gas

The production composition of fracture networks model can be analyzed with parameters in Table 2. Figure 8 shows the effect of matrix permeability of inner zone on production composition of horizontal wells with fracture networks. Higher matrix permeability of inner zone can increase flowing capacity of both free gas and desorbed gas, and accelerate spread of pressure drop in inner matrix, which is helpful for the desorption of absorbed gas.

Figure 9 shows the effect of fissure aperture of inner zone on production composition of horizontal wells with fracture
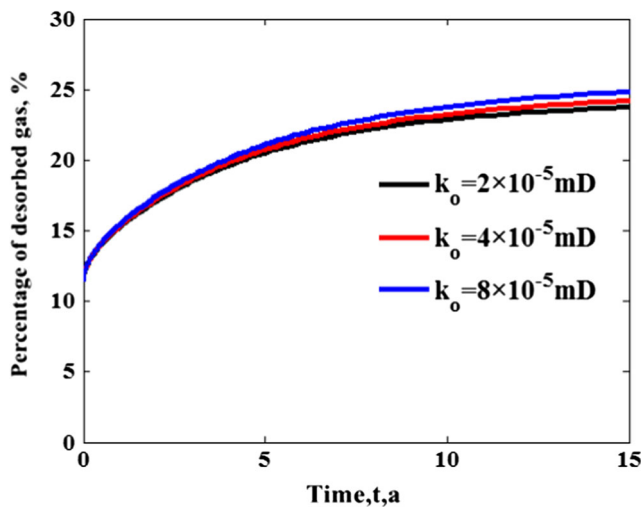

Fig. 11 The effect of matrix permeability of outer zone on production composition
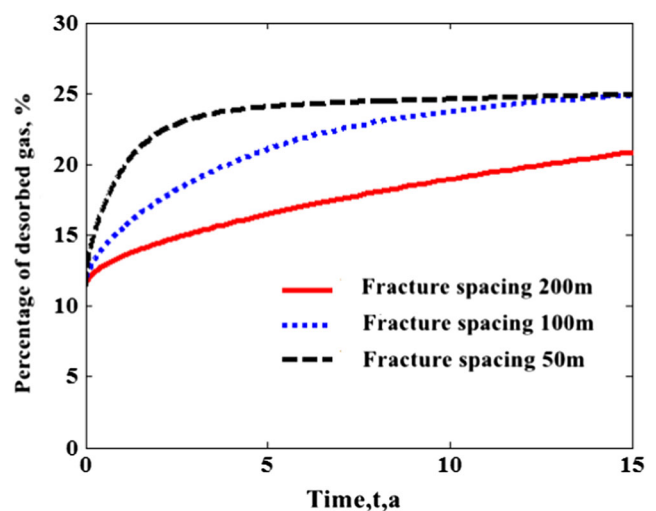

Fig. 13 The effect of induced fracture spacing on production composition

networks. Greater fissure aperture increases effective matrix permeability of inner zone and accelerates spread of pressure drop in inner matrix, which is helpful for the desorption of absorbed gas.

Figure 10 shows the effect of fissure density of inner zone on production composition of horizontal wells with fracture networks. Higher fissure density increases effective matrix permeability of inner zone and accelerates spread of pressure drop in inner matrix, which is helpful for the desorption of absorbed gas.

Figure 11 shows the effect of outer matrix permeability on production composition of horizontal wells with fracture networks. Higher matrix permeability of outer zone increases accelerates spread of pressure drop in inner matrix, which is helpful for the desorption of absorbed gas. However, the influence of matrix permeability of outer zone is less than that of inner matrix.

Figure 12 shows the effect of half-length of primary fracture on production composition of horizontal wells with fracture networks, on the condition of the same amount of secondary fractures. It is evident that half-length of primary fracture exerts great influence on production composition of fractured horizontal wells. Longer primary fracture decreases spacing of secondary fractures and helps mutual interference of secondary fractures, which has the same effect of closed boundary and results in fast drop of average pressure as well as the desorption of absorbed gas.

Figure 13 shows the effect of induced fracture spacing on production composition of horizontal wells with fracture networks on the condition of the same half-length of primary fracture. Smaller induced fracture spacing helps mutual interference of secondary fractures and facilitates the desorption of absorbed gas.

Conclusions

In this paper, we proposed an analytical model for MFHW in shale reservoirs with the consideration of secondary fractures, gas desorption, stress-sensitive fracture permeability, and pressure-dependent gas PVT properties. Based on the above analysis, the following conclusions can be obtained:

1. Based on the theory of linear flow, the model for fracture horizontal well with fracture networks in shale reservoirs is established respectively. Compared with models established formerly, production from outer zone into hydraulic fractures and stress sensitivity of hydraulic fracture are considered in the new model. What's more, dynamic productivity equations of the model are derived.
2. For fracture networks model, matrix permeability, half-length of hydraulic fractures, and spacing of hydraulic fractures will largely influence production of the well. In

addition, spacing of secondary fractures is another influence factor of productivity.
3. With the introduction of nonlinear desorption into matrix control equations, production composition of fractured horizontal shale gas wells in different moments is deeply analyzed with material balance principle and iterative method. The rank of parameters that influence the ultimate recovery is the following: half-length of hydraulic fracture > induced fracture length/hydraulic fracture spacing > hydraulic fracture spacing > conductivity of induced fractures > conductivity of hydraulic fracture > induced fracture spacing.

Nomenclature A_{cw}, cross sectional area to flow, m²; B_g, formation volume factor, rm³/sm³; c_g, gas compressibility, MPa⁻¹; c_t, total compressibility, MPa⁻¹; C_t, total compressibility of the matrix, MPa⁻¹; C_d, desorption compressibility, MPa⁻¹; G, cumulative production, 10^8m³; h, formation thickness, m; k, permeability, md; L_F, fracture space, m; M, molecular weights of gas, g/mol; ψ, pseudo-pressure, MPa²/mPa.s; λ, interporosity flow coefficient, dimensionless; ω, storativity; η_D, diffusivity ratio, dimensionless; p, pressure, MPa; p_L, Langmuir pressure, MPa; q, gas rate, m³/day; t, production time, days; t_a, pseudo-production time, days; T, formation temperature, K; V, absorbed gas volume, sm³; V_L, Langmuir volume, m³/m³; y_F, half-length of the hydraulic fracture, m; y_e, the boundary of the outer zone, m; Z, gas compressibility factor, dimensionless; ϕ, porosity, m³/m³; s_c, skin factor, dimensionless; ρ, gas density, kg/ m³; μ, fluid viscosity, mPa.s

Subscripts and superscripts D, dimensionless; F, hydraulic fracture; f, induced fracture; sc, surface condition; i, initial; o, outer zone; w, wellbore; m, matrix

References

Al-Ahmadi, H. A., & Wattenbarger, R. A. (2011). Triple-porosity models: one further step towards capturing fractured reservoirs heterogeneity. Soc Petrol Eng

Bello RO, Wattenbarger RA (2010) Modelling and analysis of shale gas production with a skin effect. J Can Petrol Technol 49(12):37–48

Brohi, I. G., Pooladi-Darvish, M., & Aguilera, R. (2011). Modeling fractured horizontal wells as dual porosity composite reservoirs - application to tight gas, shale gas and tight oil cases. Soc Petrol Eng

Bumb AC, Mckee CR (1988) Gas-well testing in the presence of desorption for coalbed methane and devonian shale. SPE Form Eval 3(1): 179–185

Chen Z, Liao X, Zhao X, Lv S, Zhu L (2016) A semianalytical approach for obtaining type curves of multiple-fractured horizontal wells with secondary-fracture networks. SPE J 21(2):538–549

Cheng L, Fang S, Wu Y, Lu X, Liu H (2017) A hybrid semi-analytical model for production from heterogeneous tight oil reservoirs with fractured horizontal well. J Petrol Sci and Eng 157:588–603

Gerami S, Darvish M, Morad K, Mattar L (2008) Type curves for dry CBM reservoirs with equilibrium desorption. J Can Petrol Technol 47(7):48–56

Guo W, Xiong W, Gao SS (2012) Experimental study on stress sensitivity of shale gas reservoirs. Special Oil Gas Reservoirs 19(1):95–97

He Y, Cheng S, Li S, Huang Y, Qin J, Hu L, Yu H (2017) A semianalytical methodology to diagnose the locations of underperforming hydraulic fractures through pressure-transient analysis in tight gas reservoir. SPE J 22(3):924–939

Huang, S., Yao, Y., Zhang, S., Ji. J., Ma. (2018). Pressure transient analysis of multi-fractured horizontal wells in tight oil reservoirs with consideration of stress sensitivity. Arab J Geosci 11: 285

Jia P, Cheng L, Huang S, Wu Y (2016) A semi-analytical model for the flow behavior of naturally fractured formations with multi-scale fracture networks. J Hydrol 537:208–220

Mayerhofer MJ, Lolon E, Warpinski NR, Cipolla CL, Walser DW, Rightmire CM (2010) What is stimulated reservoir volume? SPE Prod Oper 25(1):89–98

Mi L, Yan B, Jiang H, An C, Wang Y, John K (2017) An enhanced discrete fracture network model to simulate complex fracture distribution. J Petrol Sci and Eng 20:484–496

Ozkan E, Brown ML, Raghavan R, Kazemi H (2011) Comparison of fractured-horizontal-well performance in tight sand and shale reservoirs. SPE Res Eval & Eng 14(2):248–259

Stalgorova K, Mattar L (2013) Analytical model for unconventional multifractured composite systems. SPE Res Eval & Eng 16(3): 246–256

Tivayanonda V, Apiwathanasorn S, Economides C, Wattenbarger R (2012) Alternative interpretations of shale gas/oil rate behavior using a triple porosity model. Soc Petrol Eng. https://doi.org/10.2118/159703-MS

Wu YS, Li J, Wang C, Ding D, Di Y (2013) A generalized framework model for simulation of gas production in unconventional gas reservoirs. SPE J 19(5):845–857

Wu Y, Cheng L, Huang S, Jia P, Zhang J, Lan X, Huang H (2016) A practical method for production data analysis from multistage fractured horizontal wells in shale gas reservoirs. Fuel 186:821–829

Xu B, Haghighi M, Li X, Cooke D (2013) Development of new type curves for production analysis in naturally fractured shale gas/tight gas reservoirs. J Petrol Sci and Eng 105(1):107–115

Zhang J, Huang S, Cheng L, Xu W, Liu H, Yang Y, Xue Y (2015) Effect of flow mechanism with multi-nonlinearity on production of shale gas. J Nat Gas Sci Eng 24:291–301

Zhang L, Shan B, Zhao Y, Tang H (2018) Comprehensive seepage simulation of fluid flow in multi-scaled shale gas reservoirs. Transport Porous Med 121(2):263–288

Zhao L, Gao W, Zhao L (2013) Experiment on the stress sensitivity and the influential factor analysis of shale gas reservoirs. J Chongqing University Sci Technol (Natural Sci Edition) 3(10):43–46